PAPERS:

Deep Foundations Institute is the Industry Association of Individuals and Organizations Dedicated to Quality and Economy in the Design and Construction of Deep Foundations.

Thermal Integrity Profiling of Drilled Shafts

Gray Mullins, Ph.D., P.E., Professor, Department of Civil and Environmental Engineering, University of South Florida, Tampa, Florida, USA; gmullins@usf.edu

ABSTRACT

The construction of drilled shafts as well as other cast in place foundation alternatives relies heavily on good practices from the contractor, engineer, and inspector in order to produce a quality foundation element. As many of the installation methods involve blind concreting processes, it is difficult to be certain of an intact concrete mass of the intended dimensions. A new integrity test has been developed that provides additional insight into the integrity of drilled shaft concrete. By measuring the temperature throughout the shaft via standard access tubes, the measured temperature profile can be compared to the normal signature associated with a shaft of the specified size. This article provides an overview of the new method development, test procedure, analysis, and results.

INTRODUCTION

Drilled shafts are large-diameter cast-in-place concrete structures that can develop enormous axial and lateral capacity and consequently are the foundation of choice for many large bridges subject to extreme event loads such as vessel collisions. Drilled shafts are constructed throughout the world often using the slurry method as a means to stabilize the excavation. This means that both excavation and concreting are blind processes which increase the chances of unwittingly producing defects in the shaft.

State-of-the-art methods for evaluating the integrity of drilled shaft concrete vary where no one approach is effective in providing a full picture of the actual state of the concrete (Hertlein, 2001). Some methods are better at evaluating the core of the shaft, whereas others can best detect problems more proximal to logging/access tubes. Ideally, but not practical, a combination of all current test technologies could perhaps identify most forms of anomalies. As this is often not cost-effective, it is therefore desirable to explore other technologies that could be extended to integrity testing that may provide a more comprehensive assessment. One such concept makes use of the heat of hydration of curing concrete and temperature measurements within the shaft to assess whether or not anomalies have been formed. This type of integrity evaluation is referred to herein as Thermal Integrity Profiling or TIP.

Prior to the implementation of the new approach, heat of hydration was only viewed as an undesired side effect which has been long recognized for its potentially harmful consequences. Of the numerous case studies, the most famous is perhaps the Hoover Dam project constructed during the depression from 1932 to 1935 where over 4 million cubic meters (5.2 million cu yd) of concrete were used. At that time it was understood that staged construction and internal cooling systems would be required to help control elevated temperatures. Therein, the primary concern was concrete cracking from differential temperature and the associated tensile stresses. Without these considerations, temperature dissipation was estimated to take over 100 years and temperature-induced cracking would have severely compromised its structural integrity and its ability to prevent leakage (US Dept of Interior, 2004).

With regard to drilled shafts, these foundation elements have been routinely constructed without considering mass concrete effects and the possible long-term implications of the concrete integrity. Such considerations address the high internal temperatures that can be generated during the concrete hydration/curing phase which can be detrimental to the shaft durability and/or integrity in two ways: (1) short-term differential temperature-induced stresses that crack the concrete and (2) long-term degradation via delayed ettringite formation (Whitfield, 2006).

Understanding the parameters that affect the temperature rise in curing concrete has a two-fold benefit to the concrete and drilled shaft industry: (1) the ability to better predict the occurrence of mass concrete conditions in all concrete structures, and (2) the use of temperature generation and its diffusion to the surrounding environment to predict normal drilled shaft internal temperature distributions. This paper focuses on the latter although the

predictive computations and field measurement methods serve both needs.

BACKGROUND

Various physical, chemical, and molecular principles are combined in the concept of thermal integrity profiling of drilled shafts that address heat production in the concrete, diffusion of the heat into the soil, and the resulting temperature signature produced by a properly shaped drilled shaft (Mullins et al., 2004, 2005, 2007, and 2009; Kranc and Mullins, 2007). At various stages of the curing process these principles have more prominent effects; heat production tends to dominate the resulting temperature in the early stages whereas the surrounding dissipation process controls later on.

Heat Production. The quantity of heat and rate of heat production are directly linked to the concrete mix design and the chemical constituents of the cementitious materials. These materials are generally comprised of cement and flyash or slag. Each material produces heat when hydrating, the total magnitude of which is dependent on the cementitious fraction p (by weight) with respect to total cementitious material. The total heat, H_u, and the rate of production can be determined from equations (1) – (5) where H is in units of kJ/kg (Schindler and Folliard, 2005).

$$H_u = H_{cem}p_{cem} + 461p_{slag} + h_{FA}p_{FA} \quad (1)$$

Where the energy per kilogram of slag is directly given to be 461 kJ/kg (198 BTU/lb), the cement and flyash energy production can be determined using equations (2) and (3), respectively.

$$H_{cem} = 500p_{C_3S} + 260p_{C_2S} + 866p_{C_3A} + 420p_{C_4AF} + 624p_{SO_3} + 1186p_{FreeCaO} + 850p_{MgO} \quad (2)$$

$$h_{FA} = 1800p_{FACaO} \quad (3)$$

Both equations (2) and (3) require precise knowledge of the chemical composition of the cement and flyash in the form of the weight fraction of the various chemical compounds, p_i. These are usually available from the concrete supplier and flyash source (municipal power plant).

[TABLE 1] Effect of slag and flyash in shaft mixes on energy and duration (Eqns 1-7).

Concrete Constituents	WSDOT 4000P (Flyash)	WSDOT 4000P (Slag)	FDOT Class IV 4000 (Flyash)	FDOT Class IV 4000 (Slag)
Cement, kg (%)	276.7 (85%)	272.2 (77%)	226.8 (66%)	122.5 (39.7%)
MgO, %	0.83	1	0.7	0.9
C2S, %	13	14	10	9
C3A, %	7.1	5	7	7
C3S, %	58	60	62	63
SO3, %	2.8	2.7	2.9	2.9
C4AF, %	11.2	10	12	11.3
Blaine, m2/kg	387	411	391	386
Flyash, kg (%)	49.9 (15%)	-	114.8 (34%)	-
SO3, %	1	-	1.8	-
CaO, %	15.1	-	5.2	-
Slag, kg (%)	-	81.3 (23)	-	186.0 (60.3%)
w/cm	0.37	0.41	0.52	0.41
Energy (kJ/kg)	76.2	87.7	57.5	53.8
α	0.753	0.769	0.921	0.881
β	0.630	0.699	0.699	0.435
τ (hrs)	19.4	26.3	17.4	54.5

Schindler and Folliard (2005) further provided means to compute rate of heat production whereby curve fitting algorithms were applied to extensive laboratory studies again based on the weight fraction of the various cementitious constituents. The degree of hydration at time, t_e, can be determined using equation (4).

$$\alpha(t_e) = \alpha_u \exp\left(-\left[\frac{\tau}{t_e}\right]^\beta\right) \tag{4}$$

When α equals 1.0 all hydration energy has been developed from equation (1). The parameters α_u, β, and τ are determined again by cementitious constituent fractions, p_i, shown in equations (5) – (7), respectively, as well as the water cement ratio, w/cm.

$$\alpha_u = \frac{1.031 w/cm}{0.194 + w/cm} + 0.5 p_{FA} + 0.3 p_{SLAG} \leq 1.0 \tag{5}$$

$$\beta = p_{C_3S}^{0.227} \cdot 181.4 p_{C_3A}^{0.146} \cdot Blaine^{-0.535} \\ \cdot p_{SO_3}^{0.558} \cdot \exp(-0.647 p_{SLAG}) \tag{6}$$

$$\tau = p_{C_3S}^{-0.401} \cdot 66.78 p_{C_3A}^{-0.154} \cdot Blaine^{-0.804} \cdot \\ p_{SO_3}^{-0.758} \cdot \exp(2.187 \cdot p_{SLAG} + 9.5 \cdot p_{FA} \\ \cdot p_{FA-CaO}) \tag{7}$$

For typical shaft mixes with moderate flyash percentages (15%) τ usually is around 18-24 meaning that all energy has been expended in roughly 18 - 24 hours. High slag content mixes (e.g. 60% replacement) usually take upwards of 50 hours. Mixes with no flyash or slag are usually expended in about 15 hours. Table 1 shows the effect of using flyash or slag on approved shaft mixes from both Washington and Florida DOTs.

Heat Diffusion. Just as important as the energy production is the mechanism by which the heat is dissipated into the surrounding environment. Although the thermal integrity approach can be applied to all concrete structural elements, it is most commonly used for drilled shafts wherein the surrounding environment is largely dominated by a soil structure or geo-material.

Heat flow in soils involves simultaneous mechanisms of conduction, convection, and radiation of which conduction overwhelmingly dominates the heat transport. Conductive heat flow in soils is analogous to fluid or electrical systems. The *thermal conductivity*, λ, is defined as the heat flow passing through a unit area, A, given a unit temperature gradient, $\Delta T/L$, equation (8).

$$\lambda = \frac{q}{A \cdot \Delta T / L} \tag{8}$$

This value can be estimated by the geometric mean of the thermal conductivity of the individual matrix components: solids, water, and air. Thermal conductivity of soil minerals range from 2 to 8 W/m-C for clay to quartz, respectively. Although dependent on temperature and relative humidity, water is roughly 0.5 W/m-C and air, 0.03 W/m-C. For a saturated soil, the thermal conductivity can be determined using equation (9) where n represents the volumetric fraction of water (Johansen, 1975; Duarte et al., 2006).

$$\lambda_{sat} = \lambda_s^{(1-n)} \lambda_w^{n} \tag{9}$$

Likewise, the thermal conductivity of the solids, λs, is related to the fraction of quartz or sand, q, in the soil and is determined using equation (10). The subscript "o" denotes other soil minerals.

$$\lambda_s = \lambda_q^{q} \lambda_o^{(1-q)} \tag{10}$$

Not surprisingly, there is a strong correlation between thermal conductivity and mechanical properties as close contact / dense packing of the soil particles aides in transmitting heat by means of thermo-elastic waves. Farouki (1966) provided translation of this concept from Debye (1914) wherein heat flow through non-metallic crystalline solids occurs when warmer atoms vibrate more intensely than adjacent cooler atoms which in turn propagate waves by way of atom to atom contact at a characteristic speed. As a result, the thermal conductivity can be related to the compression wave velocity for a given material. The strength of the bonds between atoms affects this speed which is also dependent on the heat capacity of the material.

The *heat capacity* of the soil can be determined based on the volumetric fraction of solids, water, and air wherein the heat capacity of each component is defined as the heat required to raise the temperature of a unit volume of material one degree C. The heat capacity is actually the product of the mass specific heat, *c*, and the dry density of the soil, ρ. Farouki (1981) and Duarte et al. (2006) define the specific heat of a volume of soil by introducing *Xi* as the volumetric fraction of each component,

equation (11) can be used to determine the effective specific heat of the soil matrix where C_S, C_w, and C_A represent the heat capacity of the solids, water, and air, respectively.

$$C = X_S C_S + X_W C_W + X_A C_A \qquad (11)$$

In essence, two almost conflicting parameters affect heat dissipation into the surrounding soils: the ability to conduct heat (λ) and the reluctance of the soil to be heated (C). The more dense the material the better it conducts while also requiring more energy to warm. This combines into an additional parameter, the *diffusivity (k)* which is defined as the ratio of the thermal conductivity to the heat capacity, equation (12).

$$k = \frac{\lambda}{\rho \cdot c} \qquad (12)$$

For the prediction of normal internal shaft temperature, the thermal conductivity, heat capacity, and the resultant diffusivity can be determined from boring logs whereby the soil type and blow count are used to estimate mineral content and density (Pauly, 2010).

Finally, the temperature diffusion is characterized by the partial differential equation (13) where the change in temperature, T, with respect to time, t, is proportional to the product of the diffusivity, k, and the second derivative of temperature with respect to distance in three spatial directions x, y, and z.

$$\frac{\partial T}{\partial t} = k \left(\frac{\partial^2 u}{\partial x^2} + \frac{\partial^2 u}{\partial y^2} + \frac{\partial^2 u}{\partial z^2} \right) \qquad (13)$$

When a heat source, Q, is added (like concrete hydration energy) the following equation (14) governs wherein the product of the heat capacity, ρC, and the change in temperature, T, with respect to time, t, are proportional to the sum of the heat added, Q, and the divergence of the product of the conductivity, λ, and temperature gradient.

$$C \frac{\partial T}{\partial t} = Q + \nabla \cdot (\lambda \nabla T) \qquad (14)$$

This overview of heat production and dissipation provides an insight into the workings of three-dimensional finite difference algorithms that can be used to predict the temperature within the shaft at various thermal integrity testing times (Johnson and Mullins, 2007; Mullins et al., 2009). This is then coupled with shaft geometry to provide the most beneficial timeframe for performing thermal integrity profiles of the curing shaft concrete. To that end, it is important to note that these mechanics are theoretically sound and provide the reproducibility for reliable thermal integrity assessment.

CURRENT INTEGRITY TESTING PRACTICES

Most state transportation departments have adopted the Federal Highway Administration guideline for including access tubes in the reinforcing cage of drilled shafts (O'Neill and Reese, 1999). Therein, recommended tube materials, diameters, and plurality have been outlined to provide sufficient access to the shaft cross-section for non-destructive evaluation. Although originally intended for applications involving cross-hole sonic logging, CSL, or gamma-gamma logging, GGL (also called gamma density logging, GDL), this tube installation standard also provides access to measure the internal temperature of the shaft. Both CSL and GGL have a limited detection zone within the shaft cross-section: CSL is generally used to make determinations of the concrete quality directly between the tubes (inside the reinforcing cage) based on arrival times and the resultant wave speed; GGL measures the concrete density within a 76 to 114mm (3 - 4.5in) radius from the centerline of the access tube based on measured gamma counts/s (Caltrans 2005 and 2010). This leaves areas of the shaft untested. Fig. 1 shows the percentage of the cross sectional area actually tested by GGL and CSL as a function of shaft diameter based on an assumed 150 mm (6 in) cover (FDOT, 2010). The two images represent
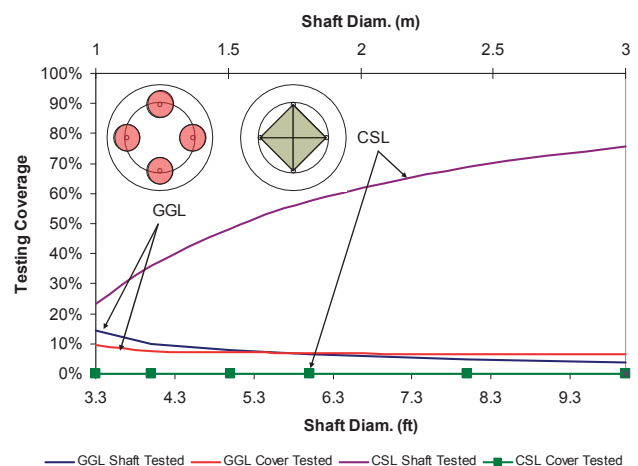
[FIG. I] Tested area of shaft cross section from **GGL** and **CSL** (150 mm or 6 in cover).

graphically the coverage when applied to a 0.9m (3ft) diameter shaft. When less cover is permitted a larger fraction of the core concrete can be assumed when using CSL testing.

Both structurally and geotechnically, the outermost concrete of the shaft provides the most benefit. The contribution to the bending capacity from the core concrete is negligible when compared to that of the outer regions where the moment of inertia is proportional to the square of the distance from the centroid to the contributing concrete area ($I = \Sigma A_i x_i^2$). In fact, recent studies have assessed the feasibility of casting shafts with a full length central void to remove the unneeded core concrete (Johnson and Mullins, 2007; Mullins et al., 2009). These sources calculate little reduction in bending capacity but recognize reductions in axial capacity (structural) roughly proportional to the fraction of the removed concrete cross section. The focus there was to reduce the peak internal temperature and the associated mass concrete conditions.

The concrete cover that forms the bond between the shaft reinforcement and the bearing strata can be considered the most important yet is only partially tested by GGL and not routinely tested by CSL without single hole methods. The thermal method of assessing shaft integrity, presented herein, is not limited to these shortcomings and is equally sensitive to anomalies both inside and outside the reinforcing cage.

METHOD DEVELOPMENT

In the wake of cone penetrometer development in the late 1970's and early 1980's, cone penetrometers were being outfitted with various sensors (e.g. pore pressure, resistivity, cameras, etc). At that time, faculty researchers at the University of South Florida gave serious consideration to taking soil temperature measurements around freshly cast shafts using the cone as the means to gain access to these regions. Two hurdles seemed insurmountable: (1) the time to achieve thermal equilibrium between a cone-based temperature sensor and the soil (without creating thermal disturbances) was too long to be practical and (2) the inability to penetrate rock or stiff soil commonly the target bearing strata. Additionally, the cost of throw-away embedded instrumentation (e.g. thermocouples or similar) in the reinforcing cage was at that time exorbitant. However, as instrumented load tests came into

favor of many designers, so did embedded inclinometer casings which opened the door to measurements from reusable down-hole devices capable of monitoring inclination, lateral acceleration, axial strain, density, wave speed, and temperature.

The first full scale versions of thermal integrity profilers used inclinometer wheel bodies with much larger infrared sensors than those used today. By the turn of the 21st century, several versions of the equipment had evolved progressively smaller to provide access in smaller diameter tubes staying abreast with the trend toward smaller CSL devices. Smaller access tubes reduce cage congestion and aid in providing better concrete flow through the cage openings. Today's probe is 32 mm (1.25 in) in diameter and 150mm (6 in) long for use in tubes as small as 38mm (1.5 in) inner diameter (Fig. 2).

THERMAL INTEGRITY PROFILING

Thermal integrity profiling uses the measured temperature generated in curing concrete to assess the quality of cast in place concrete foundations (i.e. drilled shafts or ACIP piles). The necessary information is obtained by lowering a thermal probe equipped with four horizontally-directed, infrared thermocouples (radially oriented at 0, 90, 180 and 270 degrees) into access tubes and measuring the tube wall temperature in all directions over the entire length of shaft. Throw-away embedded devices can also perform the same function given adequate quantities are used to provide sufficient coverage.
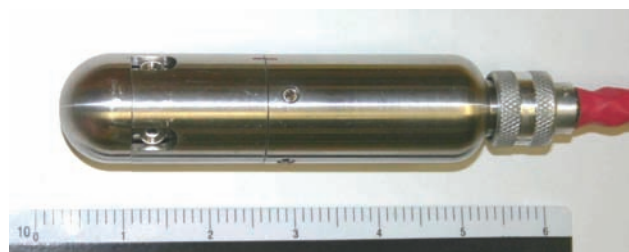
[FIG. 2] TIP probe equipped with four infrared thermocouples.

In general, the absence of intact / competent concrete is registered by relatively cool regions (necks or inclusions); the presence of additional / extra concrete is registered by relatively warm regions (over-pour bulging into soft soil strata or voids). Anomalies both inside and outside the reinforcing cage not only disrupt the normal temperature signature for the nearest access tube, but also the entire shaft; anomalies (inclusions, necks, bulges, etc.) are detected by

more distant tubes but with progressively less effect. Fig. 3 shows a thermal integrity profile being performed whereby the depth of the probe is tracked by a digital encoder wheel over which the lead wire is passed.

[FIG. 3] Thermal integrity profiler used to assess shaft concrete quality.

The internal temperature distribution across a normal cylindrical shaft is roughly bell-shaped with the effect of temperature reaching well into the surrounding soil (Fig. 4). The magnitude of the peak temperature is dependent on the concrete mix design, shaft diameter, thermal properties of the soil, and the time of hydration. However, at any time within the hydration period (and roughly the same time thereafter), a distinct, usable temperature profile exists for the given conditions. Although the magnitude of the temperature varies with time, the features (shape) of the profile do not.
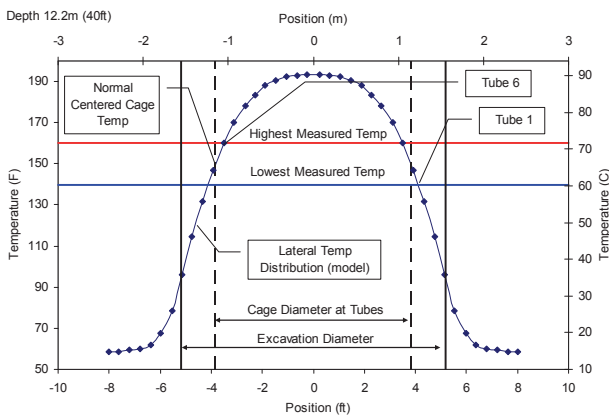

[FIG. 4] Modeled temperature distribution across a 3.3m (10ft) diameter shaft at a given depth.

CAGE ALIGNMENT

The temperature measurements from each tube are sensitive to cage eccentricity as well as the surrounding cover (effective diameter) as a function of time. Based on the temperature distribution shown in Fig. 4, the temperature in all tubes should be the same when the cage is centered. A cage slightly closer to one side of the excavation will exhibit cooler temperatures from tubes closest to the soil walls and warmer temperatures from tubes closer to the center of the shaft. Cages are often slightly off center for various reasons including: oversized excavation or casing, missing or broken spacers, bent cage, etc. Therefore a perfectly formed cylindrical shaft can exhibit higher and lower temperatures from tubes on opposite sides of the cage when the cage is not centered. By comparing both the highest tube temperature measurement and the lowest from the opposite side of the cage to the average at a given depth, cage offset can be differentiated from unwanted changes in cross section. Further, by dividing the change in temperature (from the average) by the slope of the linear portion of the modeled temperature / radius curve (Fig. 4), the magnitude of cage offset can be determined as well as the remaining concrete cover. Fig. 5 shows the results of TIP scans, for which the Fig. 4 results were modeled, showing opposite side tubes warmer or cooler than the average dependent on the amount of offset.

The data shown in Fig. 5 was collected from a 3.3m (10ft) diameter shaft (10 access tubes) constructed in Tacoma, Washington as part of the I-5 / SR16, Nalley Valley Project. By simple inspection, features of the as-built shaft geometry become recognizable. For instance, the water table was at 9.8m (32ft) and caused some sloughing before slurry was fully introduced which is seen in all tubes as being slightly warmer (bulge). The upper 4.5m (15ft) of measurements represent the access tube stick up above the top of shaft which is not of interest. The top and bottom of shaft show the normal effect of both radial and longitudinal temperature dissipation which extends a distance roughly 1 diameter down and up from the respective boundaries. At mid shaft elevations, dissipation is purely radial. Additionally, a sense of the cage alignment over the length of the shaft is obtained by comparing opposite side tubes and the change in temperature relative to the average. The amount of cage offset can be predicted as noted by Fig. 4.

The data for all tubes of the same shaft shown in Fig. 5 can be displayed for a single elevation on a radial temperature scale where warmer
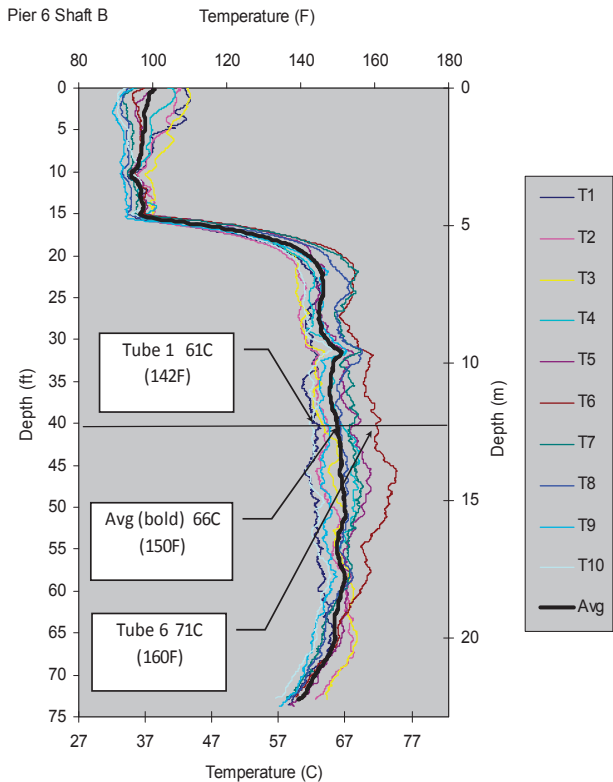
[FIG. 5] Thermal integrity data from a 3.3m (10ft) diameter shaft showing effect of cage offset on measured temperature.
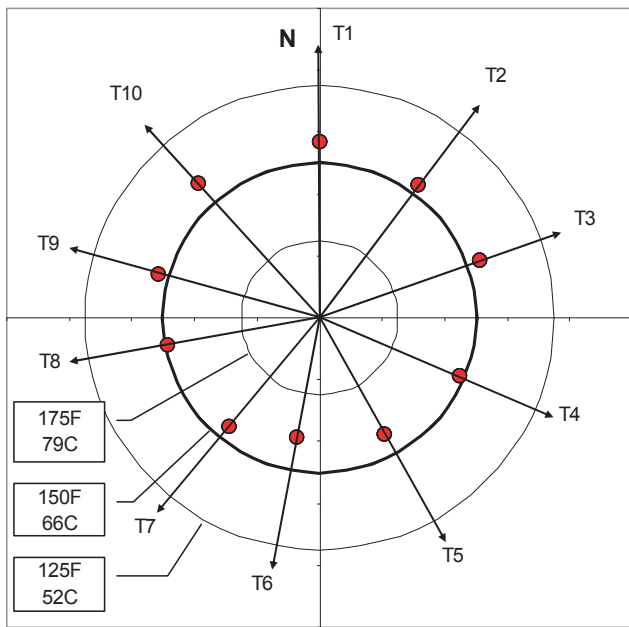

[FIG. 6] TIP data displayed on radial temperature scale from a depth of 12.2m (40ft).

tubes are plotted closest to the graph center (Fig. 6). The local temperature axes for each tube are oriented in the direction away from the center based on tube spacing and the corresponding angles. This shows that the cage is slightly north to northwest of the excavation center at that depth; a cooler measurement indicates closer proximity to the shaft edge.

SHAFT SHAPE

Concreting logs (i.e. yield plots) are a key mechanism for identifying atypical conditions. This information is collected by measuring the rise in the fluid concrete level between trucks using a weighted measuring tape. The volume of concrete from each truck and the associated rise in concrete level are compared to the theoretical volumes as a first level of post construction review / inspection and are often used to decide whether or not to perform integrity testing. When converted to the effective diameter from each truck a basic shape of the shaft can be estimated. For smaller, one or two-truck pours, no definition or shape can be defined. However, as the temperature distribution near the cage is strongly linear, the average tube temperature plotted versus depth reflects the as-built shape of the shaft. As a result, a refined rendering of the shaft can be prepared regardless of the number of trucks.

The data shown in Fig. 7 was collected from a 2.1m (7ft) diameter shaft (7 access tubes) constructed in Lake Worth, Florida as part of a Florida Turnpike widening / exit enhancement project. This shows the average temperature from all seven tubes and the concrete yield information converted to diameter as well as the planned / theoretical diameter. Note the first and last truck have not been corrected for the estimated volume required to fill the tremie and to over pour the shaft, respectively. Regardless, the diameter calculated for the
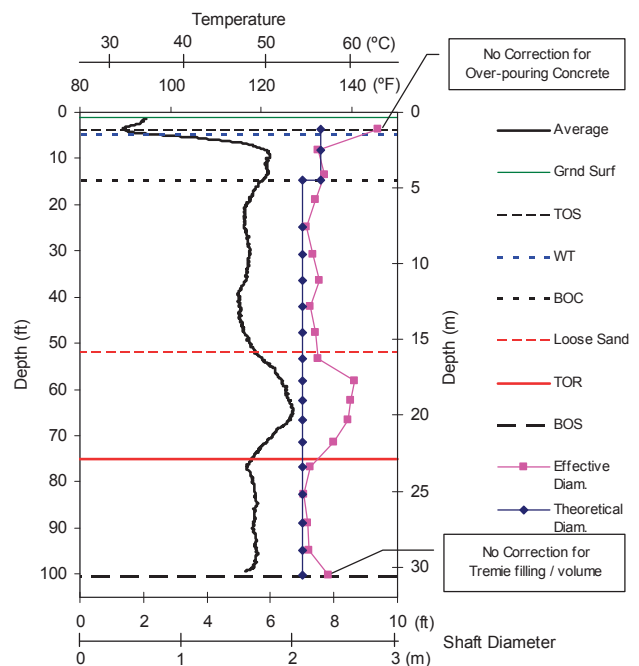
[FIG. 7] Average TIP measurements from all tubes compared with the effective diameter from construction / concreting logs.

other seventeen trucks closely correlates to the measured average temperature at those depths. In this case, a large amount of additional concrete was used due to flowing sands above the top of rock (TOR). Other construction log information is also superimposed for additional understanding of the effects on measured temperature. This includes the bottom of the temporary 2.3m (7.5ft) diameter surface casing (BOC), top and bottom of shaft (TOS and BOS), water table (WT), top of loose sand layer which continued down to top of rock (TOR) and the ground surface elevation.

The correlation between radial position and temperature (Fig. 4) in the region around the reinforcing cage coupled with the similarly strong correlation between the average tube temperatures and the as-built shaft diameter (Fig. 7) provides compelling evidence that thermal integrity profiles provide a reliable indication of the overall presence of heat producing shaft concrete. Each tube temperature profile when converted to radius can be plotted radially similar to Fig. 6 but for all depths and used to produce a 3-D rendering of the as-built shaft as shown in Fig. 8.

Just as the presence of excess concrete (higher temperatures) and proximity of the access tubes to the excavation wall (closer is cooler)

affect the measured temperature, the absence of concrete is similarly telling. Interestingly, most shafts tested exhibit over-pour features rather than necks or inclusions; however, when encountered, the lack of an intact concrete volume is also detected.

A study conducted for the Florida Department of Transportation in 2005 demonstrated the effects of cave-ins or necks on the measured temperature. Therein, a 1.2m (4ft) diameter, 7.6 m (25ft) long shaft was cast with two levels of bagged natural cuttings tied to the outside of the 0.9m (3ft) diameter reinforcing cage at depths approximate 1/3 from the top and bottom. The cross sectional loss at both levels was roughly 10 percent of the total area and was about 0.45m (1.5ft) long. At the upper level the bags were split and lumped at two locations across the shaft from each other; at the lower level all the bags were grouped together. Fig. 9 shows the results of the thermal integrity profiles taken 15 hrs after concreting and the cross section of the two anomaly levels.
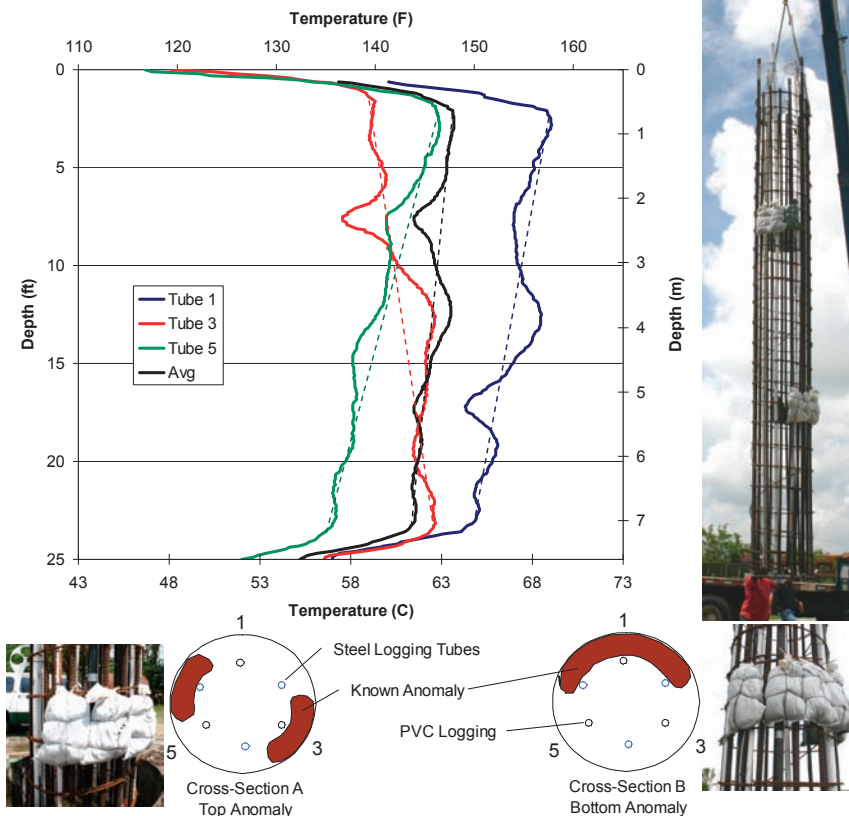
The reinforcing cage was outfitted with both steel and PVC access tubes (3 each). For convenience, tubes 1, 3, and 5 (PVC) were left dry dedicated for thermal scans while tubes 2, 4, and 6 (steel) remained flooded for CSL. Regretably, this did not provide for the normal plurality of tubes but was intended to facilitate a series of thermal scans run on 3 hr intervals.

At the upper level one group of bags was directly beside tube 3, the other was close to tube 5, and neither was adjacent to tube 1. Qualitatively, the proximity of the anomaly to the tubes is shown both by the sharpness of the change in temperature with respect to depth as well as the magnitude of change in temperature. Tube 1 shows the least temperature change
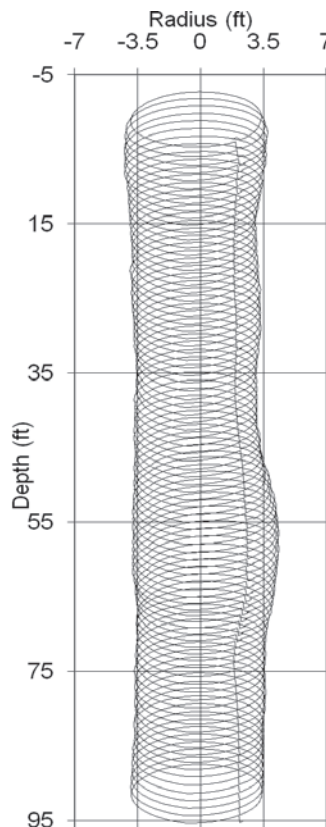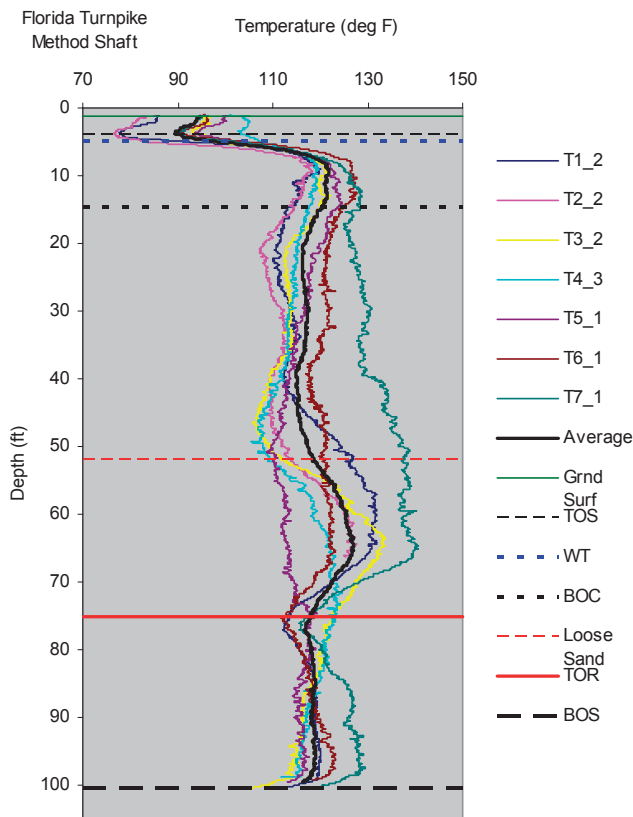
[FIG. 8] TIP data (left) converted to 3-D shape (right).

[FIG. 9] Thermal integrity profiles from 1.2m (4ft) shaft cast with known anomalies.

but the broadest disturbance. At the lower level, only tube 1 was in close proximity which showed both the sharp change in profile as well as a change in temperature with magnitude similar to tube 3 above.

Variation in temperatures between tubes again indicates poor cage alignment where at the top of shaft tube 1 starts farthest from the edge (warmest), tube 3 closest (coolest) and tube 5 very near the average (normal cover). Moving down the shaft the cover increases or decreases proportional to the measured temperature where the average represents a centered cage. The dashed lines provide a reference for a straight cage that is slightly sloped; deviations from the lines show necks or bulges. From this simplified review, when a neck in one tube corresponds to bulge on the other side, it implies the cage is deviating from straight and the cross section is not varying. For this shaft, the CSL results showed no indication of flaws but those tests were only performed using 3 and not 4 tubes.

Results of the study were used to establish thermal probe requirements, testing procedures, and preliminary analysis methods. These recommendations have been incorporated into the devices and softwares now used to perform

these tests. Full details of the study can be found elsewhere (Mullins and Kranc, 2007).

CONCLUSIONS

Over the last 30 years, the trend toward higher quality assurance in constructed drilled shafts has moved from monitoring only concrete quantities to refined slurry properties and post-construction, non-destructive testing. Where practical, the use of multiple test methods can provide more information and better assessment of shaft acceptability. Therein, no one method does it all. The thermal integrity approach provides an overall perspective of the shaft based on the presence or absence of intact heat producing concrete. The shape, cage placement, cover and concrete health are all addressed.

In the interest of space, aspects of TIP data analysis have been only briefly discussed, but several levels of analysis can be performed. These begin with a qualitative review of the temperature measurements which can identify top and bottom of shaft elevations, cage alignment, and gross section changes. When construction and concreting logs are included correlations between diameter and temperature can be established which verify the final location of the poured concrete volume. The majority of TIP results do not require modeling to be interpretted; rather, an understanding of the normal temperature profiles and features is necessary. However, results of numerical modeling can be directly compared to field measurements using the recent advancements in hydration energy predictions for modern concrete constituents. To this end, signal matching model results to field measurements can be used to determine the extent and magnitude of anomalous regions. Such comparisons additionally serve to verify the proper hydration process.

As with other test methods thermal integrity profiles identify a normal baseline temperature; GGL and CSL identify a normal baseline gamma count or arrival time, respectively. From these measurements physical parameters are

estimated (density, GGL; compression wave velocity, CSL). TIP measurements verify the presence of curing cementitious materials from which a volume of intact concrete is estimated. Consequently, predictions of normal density, velocity, or temperature can be made prior to or after testing as a measuring stick of normalcy but in reality local variations from the shaft norm are more reasonable and practical. This is often the mode of evaluation for thermal testing as well.

LIMITATIONS

Thermal integrity profiling requires temperature generation from hydrating materials to provide distinction between cementitious and non-cementitious materials. Testing should be performed while these materials are warm enough to establish a usable temperature gradient which ranges from 2 to 10 days depending on shaft diameter (roughly proportional to shaft diameter in feet, respectively).

When thermal modeling is used as the comparative basis for shaft acceptance, verification of mill certifications from the concrete supplier (constituent fractions) may be necessary as the most common method used by industry to establish constituent percentages are not exact tests. As a result, field validation of model predicted time versus temperature relationships can be performed by simple shaft temperature monitoring using small inexpensive thermocouple data collectors. Thermal integrity profiling using multiple embedded sensors can provide data for both purposes.

Thermal integrity profiling can be performed in both PVC and steel access tubes. However, if tubes are filled with water during construction, the water must be expelled prior to testing, stored, and returned after testing if CSL tests are to be conducted. If CSL tests are not planned, water is not necessary during construction as TIP results are not sensitive to debonding and the water is not used.

DISCLOSURE

This technology was developed by the University of South Florida, for which the author is an active researcher and faculty member. As is customary with such developments, the principal investigators were named as the inventors, and the university has licensed this technology to an outside firm, FGE, LLC, who has in turn teamed with PDI to manufacture the equipment. The author serves as a part-time consultant for FGE in keeping with guidelines set forth by the University Collective Bargaining Agreement.

ACKNOWLEDGMENTS

REFERENCES

1. Caltrans, 2005. Method of ascertaining the homogeneity of concrete in cast-in-drilled-hole (CIDH) piles using the gamma-gamma test method. California Department of Transportation Specifications, California Test 233.

2. Caltrans, 2010. Gamma-gamma logging (GGL). http://www.dot.ca.gov/hq/esc/geotech/ft/gamma.htm

3. Debye, P., 1914. Vorträge über die kinetische theorie der materie und der elektrizität (trans. Discussion of Kinetic Theory of Matter and Electricity), gehalten in Göttingen auf einladung der Kommission der Wolfskehlstiftung, B.G. Teuber Publisher, Liepzig and Berlin.

4. Duarte, A., Campos, T., Araruna, J., and Filho, P., 2006. Thermal properties of unsaturated soils. *Unsaturated Soils*, GSP, ASCE, pp. 1707-1718.

5. FDOT, 2010. Standard specifications for road and bridge construction. Florida Department of Transportation, ftp://ftp.dot.state.fl.us/LTS/CO/Specifications.

6. Farouki, O., 1966. Physical properties of granular materials with reference to thermal resistivity. Highway Research Record 128, National Research Council, Washington, DC, pp 25-44.

7. Farouki, Omar T., 1981. Thermal properties of soils. CRREL Monograph 81-1, Army Corps of Engineers Cold Regions Research and Engineering Laboratory, Hanover, New Hampshire.

8. Hertlein, B., 2001. Are our client's expectations realistic? Geo-Strata, Geo-Institute of the American Society of Civil Engineers, January, p.11.

9. Johansen, O., 1975. Thermal conductivity of soils and rocks. *Proceedings of the Sixth International Congress of the Foundation Francaise d'Etudes Nordigues*, Vol. 2, pp.407-420.

10. Johnson, K. and Mullins, G., 2007. Concrete temperature control via voiding drilled shafts. *Contemporary Issues in Deep Foundations*, ASCE Geo Institute, GSP No.158, Vol. I, pp. 1-12.

11. Kranc, S.C. and Mullins, G., 2007. Inverse method for the detection of voids in drilled shaft concrete piles from longitudinal temperature scans. Inverse Problems Design and Optimization Symposium, Miami, FL, April 16-18, 2007.

12. Mullins, A. G. and Kranc, S. C., 2004. Method for testing the integrity of concrete shafts. US Patent 6,783,273.

13. Mullins, G. and Ashmawy, A., 2005. Factors affecting anomaly formation in drilled shafts. Final Report, FDOT Project BC353-19, March.

14. Mullins, G. and Kranc, S., 2007. Thermal integrity testing of drilled shafts. Final Report, FDOT Project BD544-20, May.

15. Mullins, G., Winters, D., and Johnson, K., 2009. Attenuating mass concrete effects in drilled shafts. Final Report, FDOT Project BD544-39, September, 148 pp.

16. O'Neill, M.W. and Reese, L. C., 1999. Drilled shafts: construction procedures and design methods. U.S. Department of Transportation, Publication No. FHWA-IFF-99-025, ADSC-TL 4, Volume II.

17. Pauly, N., 2010. Thermal conductivity of soils from the analysis of boring logs. Master's Thesis, University of South Florida Department of Civil and Environmental Engineering, December.

18. Schindler, A. and Folliard, K., 2005. Heat of hydrations models for cementitious materials. *ACI Materials Journal*, Vol. 102, No.1, pp. 24-33.

19. U.S. Department of the Interior, 2004. Story of Hoover Dam; concrete. Bureau of Reclamation, http://www.usbr.gov/lc/hooverdam/History/essays/concrete.html.

20. Whitfield, T., 2006. "Effect of C3S content on expansion due to ettringite formation. Master's Thesis, University of South Florida Department of Civil and Environmental Engineering, June.